

# Modeling Transient Discharge into a Tunnel Drilled in a Heterogeneous Formation

by Pierre Perrochet<sup>1</sup> and Antonio Dematteis<sup>2</sup>

---

## Abstract

An analytical model is developed to predict transient discharge flow into a tunnel drilled at various speeds through a heterogeneous formation. This model relies on simplifying assumptions commonly enforced in hydrogeologic engineering, and combines the convolution and superposition principles to account for composite sections with arbitrary parametric contrasts. An application to the data monitored during the exploratory drilling of an Alpine tunnel confirms the validity of the approach.

---

## Introduction

One of the key design and safety issues to address before excavating a tunnel in deep, saturated geological formations is a realistic evaluation of the ground water discharge rates that may be generated during the drilling process and beyond. Such predictions are generally attempted either by means of numerical simulators (e.g., Anagnostou 1995; Molinero et al. 2002) or, more rapidly, by analytical solutions based on idealized flow configurations. This latter approach is considered here, as it is often preferred in practice for first estimations and parametric sensitivity analysis.

A large variety of formulae have been developed to predict tunnel discharge rates under various typical flow configurations and boundary conditions. However, these analytical solutions yield either relatively small, steady-state final values (e.g., Goodman et al. 1965; Chisyaki 1984; El Tani 2003) or unrealistically high, transient-state initial values (e.g., Maréchal and Perrochet 2003; Perrochet 2005a; Renard 2005) due to the assumption of instant tunnel activation over its whole length. Moreover, these well-known solutions generally assume homogeneous geologic materials.

In reality, tunnels are commonly drilled through highly heterogeneous and fractured formations. Discharge is initially zero and evolves in a succession of flood and recession patterns, featuring local maxima dictated by the hydrogeologic properties of the rocks encountered along the tunnel axis, as well as by the drilling speed. A convolution integral was recently developed (Perrochet 2005b) to evaluate transient inflows into homogeneous tunnels of finite length and to analyze their sensitivity to the drilling speed by means of type curves. Combining this approach with the superposition principle, this paper extends the analysis to tunnels gradually drilled through heterogeneous formations and provides an application example based on field data.

## Homogeneous Case

The base case of a deep tunnel drilled through a radially infinite, homogeneous aquifer of finite thickness was addressed in detail in a previous paper (Perrochet 2005b). It is illustrated in Figure 1a and is briefly recalled subsequently. Assuming hydrostatic initial conditions, constant drilling speed, semiinfinite radial-flow symmetry, and no significant piezometric perturbations ahead of the drilling front, the specific discharge at any drilled location can be expressed by:

$$q(x, t) = \frac{2\pi Ks}{\ln \left[ 1 + \sqrt{\frac{\pi K}{Sr^2} \left( t - \frac{x}{v} \right)} \right]}, \quad t - \frac{x}{v} > 0 \quad (1)$$

where the symbols stand for hydraulic conductivity ( $K$ ), specific storage coefficient ( $S$ ), drawdown at the tunnel

---

<sup>1</sup>Corresponding author: Centre of Hydrogeology, University of Neuchâtel, 2000 Neuchâtel, Switzerland; <http://www.unine.ch/chyn/>; pierre.perrochet@unine.ch

<sup>2</sup>SEA Consulting, Via Cernaia 27, 10121 Torino, Italy; dematteis@seaconsult.it

Received November 2006, accepted May 2007.

Copyright © 2007 The Author(s)

Journal compilation © 2007 National Ground Water Association.  
doi: 10.1111/j.1745-6584.2007.00355.x

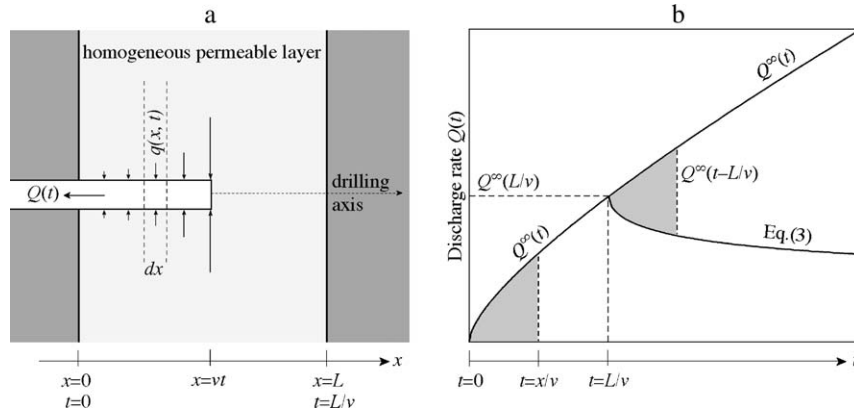


**Figure 1. Tunnel drilled through a subvertical permeable layer. (a) Nonuniform specific discharge resulting from progressive drilling. (b) Transient discharge  $Q(t)$  as expressed in Equation 3 with maximum at  $t = L/v$ .**

( $s$ ), drilling speed ( $v$ ), tunnel radius ( $r$ ), time ( $t$ ), and spatial coordinate along the tunnel axis with an origin at the entry of the permeable zone ( $x$ ). The total discharge into the tunnel during and after its excavation is thus obtained by the convolution integral:

$$Q(t) = 2\pi \int_0^{vt} \frac{KsH(L-x)}{\ln\left[1 + \sqrt{\frac{\pi K}{Sr^2} \left(t - \frac{x}{v}\right)}\right]} dx \quad (2)$$

where  $L$  is the length over which the tunnel intersects the permeable zone. In the preceding equation, the use of the Heaviside step-function  $H(u)$  ( $H(u) = 1, u > 0$  and  $H(u) = 0, u < 0$ ) is meant to prevent the occurrence of new inflows as soon as the drilling front passes beyond the distance  $L$  (from time  $L/v$  onward).

The cumulative integral in Equation 2 indicates that transient total discharge monotonically increases from the initial time to the drilling time  $L/v$  where a maximum is reached. At later times, the total discharge monotonically decreases since the drilling of the permeable zone has been completed. As suggested in Perrochet (2005b), and considering the two equal-size shaded areas in Figure 1b, the temporal evolution of  $Q(t)$  corresponds to the superposition of two identical tunnels of infinite length, each producing the discharge  $Q^\infty(u)$ , with the second tunnel activated with negative drawdown after the drilling time  $L/v$ . Performing the integral in Equation 2 indeed results in:

$$Q(t) = Q^\infty(t) - H\left(t - \frac{L}{v}\right) Q^\infty\left(t - \frac{L}{v}\right) \quad (3)$$

$$Q^\infty(u) = 4Sr^2sv[\text{Ei}(2X) - \text{Ei}(X) - \ln(2)], \quad (4)$$

$$X = \ln\left(1 + \sqrt{\frac{\pi K}{Sr^2} u}\right)$$

where Ei is the exponential integral function.

In practice, the time during which these equations may hold is not infinite but is limited by the time  $t_{\text{lim}}$  needed for the drawdown perturbation to reach an aquifer

boundary (e.g., impervious layer, surface water body) at a radial distance  $R$  from the tunnel axis. For relatively large, idealized systems, this limiting time can be evaluated by:

$$t_{\text{lim}} \approx \frac{1}{8} \frac{SR^2}{K} \quad (5)$$

For larger times ( $t > t_{\text{lim}}$ ), the specific discharge occurring at drilled locations  $x < v(t - t_{\text{lim}})$  starts to be gradually influenced by possible boundary effects and Equation 2 gradually loses accuracy. Its use, however, is well suited to aquifers of small diffusivities ( $K/S$ ) and/or deep tunnels (large  $R$ ).

### Heterogeneous Case

The two-component superposition applied in Equation 3 yields the transient discharge rate during and after the drilling of a single, homogeneous, permeable sector of length  $L$ . Considering now  $N$  consecutive sectors as schematized in Figure 2, each of them characterized by

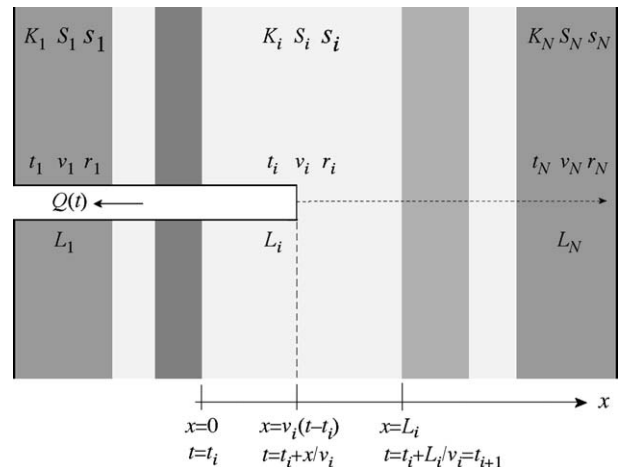


**Figure 2. Schematic of a tunnel progressively drilled through a subvertical multilayered system. Sector parameters and local drilling coordinates.**

specific parameters, the discharge rate produced by the  $i$ th sector can be straightforwardly generalized to:

$$Q_i(t) = H(t - t_i)Q_i^\infty(t - t_i) - H(t - t_{i+1})Q_i^\infty(t - t_{i+1}), \quad t > 0 \quad (6)$$

$$Q_i^\infty(u) = 4S_i r_i^2 s_i v_i [\text{Ei}(2X_i) - \text{Ei}(X_i) - \ln(2)],$$

$$X_i = \ln\left(1 + \sqrt{\frac{\pi K_i}{S_i r_i^2} u}\right) \quad (7)$$

In these equations, the hydrogeologic ( $K_i$ ,  $S_i$ ,  $s_i$ ) and drilling ( $t_i$ ,  $v_i$ ,  $r_i$ ) parameters are identified for each sector by the indice  $i$ , where  $t_i$  is the drilling time at the entry of the  $i$ th sector, defined by:

$$t_i = \sum_{j=1}^{i-1} \frac{L_j}{v_j}, \quad t_1 = 0 \quad (8)$$

with  $t_{N+1}$  as the total drilling time.

Summing up the transient contribution of each sector expressed in Equation 6 yields the total discharge at time  $t$ , during and after the drilling of the entire tunnel, namely:

$$Q(t) = \sum_{i=1}^N H(t - t_i)Q_i^\infty(t - t_i) - H(t - t_{i+1})Q_i^\infty(t - t_{i+1}) \quad (9)$$

This result can also be expressed under the nonintegrated form:

$$Q(t) = 2\pi \sum_{i=1}^N H(t - t_i) \times \int_0^{v_i(t-t_i)} \frac{K_i s_i H(L_i - x)}{\ln\left[1 + \sqrt{\frac{\pi K_i}{S_i r_i^2} \left(t - t_i - \frac{x}{v_i}\right)}\right]} dx \quad (10)$$

which corresponds to the heterogeneous version of Equation 2 and where the integrand has a local origin ( $x = 0$ ) at the entry of the  $i$ th sector.

### Field Example

The Modane exploratory tunnel is located in the French Western Alps and is part of the geologic investigation program of the Lyon-Turin high-speed railway project. This tunnel is excavated in metamorphic rocks belonging to a Permian-Triassic sequence of the so-called "Brianzonese Zone." These rocks are crossed by subvertical fault zones that are intensely fractured and more permeable than the neighboring rock-mass. The fault zones typically include a central zone composed of cataclasites and tectonic breccias, with a thickness ranging from some centimeters to a few meters, bounded by a strongly fractured zone (more than 25 joints/m) with a total thickness of up to 10 m.

Many data were collected during the excavation of the tunnel. Cumulative water discharge measurements were

done by means of three electronic weirs located at the entrance of the tunnel, as well as at 400 m and at 600 m from the portal. The first 611 m of the tunnel were almost completely excavated in quartzite, except for three major fault zones, where carbonate rocks (named "cagneules" in the Alpine literature) and mylonitic marbles were encountered. Such carbonate rocks are extremely weak, locally affected by dissolution phenomena increasing their permeability. The quartzites have a massive texture with poorly defined foliation and with pervasive fractures. These fractures were probably generated by fault-related tectonic stress fields, and by more recent superficial stress releases associated with the geomorphological evolution of the mountain slopes. From 611 m onward, the tunnel again crosses a sequence of cagneules, including quartzite clasts associated with a fault zone.

The available drilling data cover a period of 475 d corresponding to a penetration distance of 760 m. They essentially consist of daily discharge rates, along with the distance drilled every day and succinct geologic information. These data indicate that sustained inflows gradually take place after 89 d of drilling, at a distance of 191 m. Beyond this distance, the predrilling piezometric level above the tunnel increases because the tunnel penetrates deeper beneath the mountain and deeper below the water table. The piezometric levels increase from a few meters to about 105 m above the tunnel axis. At drilled locations (assumed at atmospheric pressure), this piezometric level represents the hydraulic drawdown  $s$ . During the remaining 386 d, drilling speeds of a few meters per day are recorded and there are a number of stops, or drastically reduced progression, at the intersection with sometimes very short productive fault zones. The tunnel radius is 5 m.

On the basis of this detailed drilling history, the analytical solution in Equation 9 is applied in an attempt to simulate the daily discharge rates monitored at the tunnel portal. Two modeling strategies are explored. The first one (model 1) is simplified and is based on 10 tunnel sectors, each corresponding to the type of geologic materials encountered. The second one (model 2) is more refined and includes 180 sectors, each corresponding to the progression recorded during the days of uninterrupted active drilling.

### Model 1

The hydrogeologic and drilling data for the 10 tunnel sectors considered in the simplified model are summarized in Table 1.

For each sector  $i$ , the length ( $L_i$ ), the initial and final drilling times ( $t_i$  and  $t_{i+1}$ ), and the saturated zone thickness ( $s_i$ ) above the tunnel axis are directly observed in the field. The drilling speed ( $v_i$ ) can therefore be calculated for each sector. Given that the excavation process of a given sector was periodically stopped or relaxed, this drilling speed reflects an average, uniform progression. The values indicated for the hydraulic conductivity ( $K_i$ ) and specific storage coefficient ( $S_i$ ) are those identified by calibration, indicating sector hydrodynamic diffusivities of either  $10^{-5}$  m<sup>2</sup>/s (quartzites) or  $10^{-4}$  m<sup>2</sup>/s (cagneules) or  $5 \times 10^{-4}$  m<sup>2</sup>/s (marbles). To preserve hydrogeologic consistency during the calibration process, the

**Table 1**  
**Parametric and Geologic Information for the 10 Sectors Considered in the Simplified Model**

Sectors	$L_i$ (m)	$t_i$ (d)	$t_{i+1}$ (d)	$v_i$ (m/d)	$s_i$ (m)	$K_i$ (m/s)	$S_i$ (1/m)	Geology
1	191	0	89	2.1	5	$10^{-8}$	$10^{-3}$	Quartzites
2	160	89	170	2.0	25	$10^{-6}$	$10^{-1}$	Quartzites with carginieules
3	14	170	199	0.5	75	$10^{-5}$	$10^{-1}$	Carginieules and faults
4	6	199	203	1.5	75	$5 \times 10^{-5}$	$10^{-1}$	Mylonitic marbles and faults
5	35	203	222	1.8	75	$10^{-8}$	$10^{-3}$	Quartzites
6	52	222	231	5.8	75	$10^{-6}$	$10^{-1}$	Quartzites and faults
7	153	231	292	2.5	75	$10^{-8}$	$10^{-3}$	Quartzites
8	36	292	377	0.4	105	$10^{-6}$	$10^{-1}$	Quartzites with carginieules
9	9	377	382	1.8	105	$10^{-5}$	$10^{-1}$	Carginieules and faults
10	104	382	475	1.1	105	$10^{-8}$	$10^{-3}$	Quartzites

same values were applied to sectors of similar geologic type, finally yielding satisfactory results.

Figure 3 shows a comparison between the observed discharge rates and those simulated using the calibrated hydrogeologic parameters. The gradual contributions and the averaging properties of each of the 10 model sectors are clearly shown in this diagram. Characterized by uniform equivalent parameters, these few successive sectors are obviously unable to capture some of the observed local and short-term flow spikes. This drawback, however, does not prevent the simulated results from being compatible with the overall discharge trends measured over the whole drilling period. The three maxima in the range 160 to 180 L/s detected over the explored distance, for example, are reproduced with excellent practical accuracy.

#### Model 2

The refined model starts with the first productive formation encountered at 191 m from the tunnel portal at day 89 (start of sector 2 in model 1). The remaining 569 m of

tunnel are represented by 180 consecutive sectors, each corresponding to the progression during the periods of uninterrupted active drilling. The complete data set (too large to give here) features typical sector lengths in the range 1 to 10 m and active drilling speeds from 0.4 to 8.5 m/d. During the observed discharge period, from day 89 to day 475, there are 200 d of active drilling and 186 d where drilling is on standby.

After calibration, hydraulic conductivities and specific storage values, respectively, in the range  $10^{-6}$  to  $10^{-4}$  m/s and  $10^{-2}$  to  $10^{-1}$  1/m, are assumed in the productive faulted sectors, while much less permeable sectors are assumed to have  $K$  and  $S$  values on the order of  $10^{-9}$  m/s and of  $10^{-3}$  1/m. As shown in Figure 4, the modeled transient discharge rates again compare fairly well with those measured in the field. Local flood-recession events of various magnitudes are well reproduced, with recession phases due either to further penetration into a sector with low permeability or to a stop of the drilling process.

Compared to the simplified model based on only 10 sectors with averaged hydrogeologic and drilling

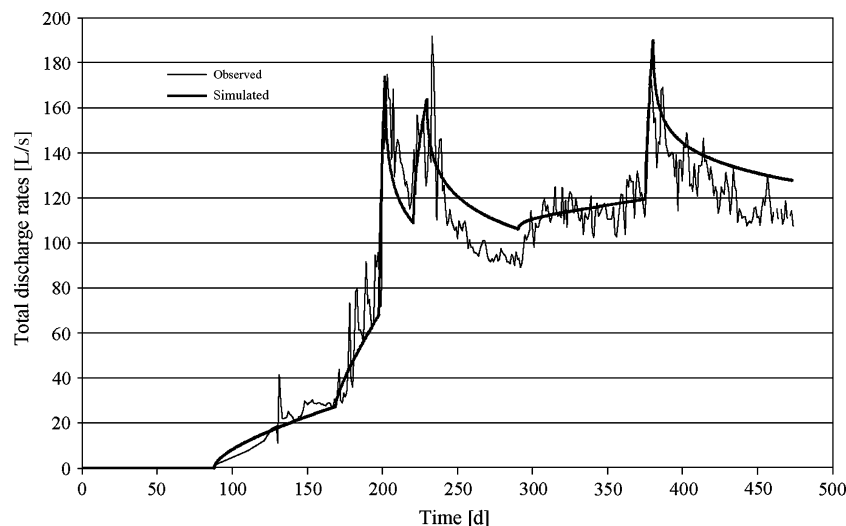


**Figure 3. Discharge rates into the Modane exploratory tunnel. Comparison of observed values with the analytical simulation using the simplified model (model 1, 10 sectors).**

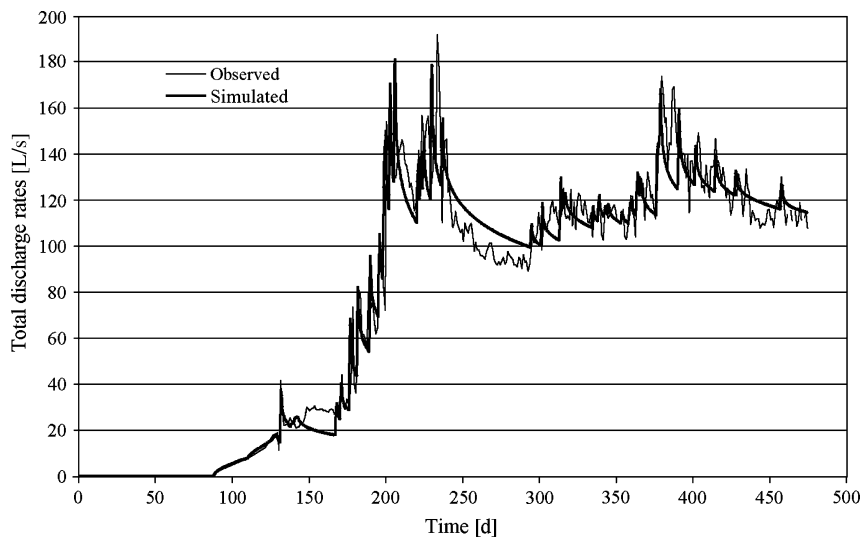


**Figure 4. Discharge rates into the Modane exploratory tunnel. Comparison of observed values with the analytical simulation using the detailed drilling history (model 2, 180 sectors).**

parameters (model 1, Figure 3), the refined model accounts for a large number of local structures and discontinuities (fractures and faults) contributing to the total ground water discharge by a cumulated series of local flow spikes, as is generally expected in the tunneling context. In the present example, these improved model features certainly look more realistic. However, they may not provide fundamentally new insights as to the overall evolution of the drainage process or the maximum discharge rates indicated by the simplified model. Nevertheless, the results obtained with this detailed model confirm the validity and the flexibility of the approach to handle cases of higher hydrogeologic complexity.

## Conclusions

A relatively simple approach is proposed to explain the high variability of the discharge rates drained by a tunnel progressively drilled through a heterogeneous series of subvertical layers. The *a posteriori* performances of the analytical solution developed in this paper are demonstrated in the case of an Alpine tunnel for which daily drilling data and discharge rates are available. Two models are considered, one with a coarse and one with a very detailed parameterization, both yielding good results.

However, the use of such models for *a priori* discharge predictions must be made very carefully. As in any other ground water flow simulation method, the definition of input geologic features and dynamic properties remains the major limiting factor. The application of this approach for tunnel discharge forecasting should therefore always be associated to a reliability analysis of the hydrogeologic conceptual model.

## Acknowledgments

The authors thank the company Lyon Turin Ferroviare SAS for providing the data. The comments of three anonymous reviewers were greatly appreciated.

## References

- Anagnostou, G. 1995. The influence of tunnel excavation on the hydraulic head. *International Journal for Numerical and Analytical Methods in Geomechanics* 19, no. 10: 725–746.
- Chisyaki, T. 1984. A study of confined flow of ground water through a tunnel. *Ground Water* 22, no. 2: 162–167.
- El Tani, M. 2003. Circular tunnel in a semi-infinite aquifer. *Tunnelling and Underground Space Technology* 18, no. 1: 49–55.
- Goodman, R.F., D.G. Moye, A. Van Schaikwyk, and I. Javandel. 1965. Ground water inflows during tunnel driving. *Bulletin of the International Association of Engineering Geologists* 2, no. 1: 39–56.
- Maréchal, J.C., and P. Perrochet. 2003. New analytical solution for the study of hydraulic interaction between Alpine tunnels and ground water. *Bulletin de la Société Géologique de France* 174, no. 5: 441–448.
- Molinero, J., J. Samper, and R. Juanes. 2002. Numerical modeling of the transient hydrogeological response produced by tunnel construction in fractured bedrocks. *Engineering Geology* 64, no. 4: 369–386.
- Perrochet, P. 2005a. A simple solution to tunnel or well discharge under constant drawdown. *Hydrogeology Journal* 13, no. 5–6: 886–888.
- Perrochet, P. 2005b. Confined flow into a tunnel during progressive drilling: An analytical solution. *Ground Water* 43, no. 6: 943–946.
- Renard, P. 2005. Approximate discharge for constant head test with recharging boundary. *Ground Water* 43, no. 3: 439–442.